International Communications in Heat and Mass Transfer 39 (2012) 1054–1058

Contents lists available at SciVerse ScienceDirect

International Communications in Heat and Mass Transfer

journal homepage: www.elsevier.com/locate/ichmt

Experimental investigation of thermoelectric power generation versus coolant pumping power in a microchannel heat sink☆

A. Rezania *, L.A. Rosendahl, S.J. Andreasen

Department of Energy Technology, Aalborg University, DK-9220 Aalborg, Denmark

ARTICLE INFO

Available online 20 July 2012

Keywords:
Thermoelectric generators
Pumping power
Microchannel heat sink
Experimental investigation

ABSTRACT

The coolant heat sinks in thermoelectric generators (TEG) play an important role in order to power generation in the energy systems. This paper explores the effective pumping power required for the TEGs cooling at five temperature difference of the hot and cold sides of the TEG. In addition, the temperature distribution and the pressure drop in sample microchannels are considered at four sample coolant flow rates. The heat sink contains twenty plate-fin microchannels with hydraulic diameter equal to 0.93 mm. The experimental results show that there is a unique flow rate that gives maximum net-power in the system at the each temperature difference.

1. Introduction

In the power generation systems, a key factor is the optimization of the systems design, together with its heat source and heat sink. In the case of the thermoelectric generators (TEG), for increasing the convective surface area, in order to provide high density of heat dissipation at the surface of the structure, microscale heat transfer systems can enhance the thermal coupling to the hot and cold reservoirs [1]. Therefore, the challenge is to design an effective heat exchanger within microelectronic dimension restrictions [2]. Microscale single-phase heat transfer has been widely used in industrial and scientific applications [3]. Using microchannel heat sinks provides low weight and compact energy systems, compared to the traditional macroscale heat sinks, and increases modularity. In contrast to macrochannels, a reduced flow rate in the microchannel heat sink is sufficient to maintain the same average temperature difference between the hot and cold sides of the TEGs. Using microchannel heat sinks also increases the Nusselt number in the channels [4].

In microchannels, the convective heat transfer increases at the high relative roughness of the channel walls, so that the critical Reynolds number changes with the wall roughness in a different way compared to the typical macrochannels. There are observations of earlier transition from laminar to turbulent flow regime in microchannels compared to the macrochannels theory [5,6]. The earlier transition happens at lower Reynolds number when the hydraulic diameter of the microchannel decreases [7,8]. The studies indicate that, the geometric configuration of the microchannel heat sinks has a critical effect on the convective heat transfer of the laminar flow in the heat sink [9]. In order to achieve overall heat transfer enhancement a rectangular microchannel is the best shape, and its heat transfer coefficient is the highest amongst trapezoidal and triangular shaped microchannels [10].

A comparison of thermal efficiencies is conducted with triangular, rectangular and trapezoidal microchannels with the same hydraulic diameter by Chen et al. [11]. Their results show that the cross-sectional shape has a significant effect on the temperature distribution of heat sinks, and the lowest pumping power is required for the triangular microchannel heat sink. Kroeker et al. [12] found that, on the basis of equal hydraulic diameter and equal Reynolds number, a rectangular channel has less thermal resistance compared with heat sinks with circular channel. Additionally, the laminar friction factor or flow resistance reaches a minimum value as the channel aspect ratio approaches 0.5 [9]. As reported by Tuckerman and Pease [13], when the channel width and the fin thickness are equal, the heat sink gives the minimum thermal resistance. The inlet/outlet plenum effect gives a non-uniform velocity and flow rate distribution in each channel under a given pressure drop in the heat sink, so that a non-uniform temperature distribution happens in the heat sink [14]. The heat sinks with the vertical coolant supply and collection via inlet and outlet ports of the heat sink provide better uniformities in temperature and velocity, so that this type of heat sink can make better performance due to smaller thermal resistance among the studied heat sinks.

The heat exchanger designs have mostly disconnected to the higher performance TEGs. The development work mostly focused on thermoelectric materials required a significant amount of engineering parametric analysis. Since, the ZT of the thermoelectric materials is not the only factor to improve the output power of the system, the whole parts of the energy conversion system, such as thermal contacts of the hot and cold heat exchangers, needed to be considered. The thermal resistances of the heat exchangers have a strong influence on the

☆ Communicated by W.J. Minkowycz.

* Corresponding author.
E-mail address: alr@et.aau.dk (A. Rezania).

0735-1933/$ – see front matter © 2012 Elsevier Ltd. All rights reserved.
doi:10.1016/j.icheatmasstransfer.2012.07.010

Nomenclature

A	TEG leg area, m^2
C_p	specific heat of water, 4178 J/kg.K
D	diameter, m
D_h	hydraulic diameter of the channel, m
H	height, m
I	current, A
L	length, m
$\dot{m}$	mass flow rate, kg/s
P	power, W
p	pressure, Pa
Pr	Prandtl number
Re	average Reynolds number
Q	heat absorbed by heat sink, W
T	temperature, K
t	heat sink wall thickness, m
u	coolant flow velocity in the microchannel, m/s
V	voltage, V
$\dot{V}$	volumetric flow rate, m^3/s
w	width, m
x_h	thermal entry length, m

Greek symbols

α	Seebeck coefficients, V/K
Δ	value difference
μ	water dynamic viscosity, $N.s/m^2$
ρ	water density, kg/m^3

Subscripts

av	average
ch	microchannel
hs	heat sink
i	inlet
n	net
o	outlet
p	pump
pl	plenum
teg	thermoelectric generator

electric power produced by the TEG. Martinez et al. [15] optimized the heat exchangers of a TEG in order to maximize the electric power generated by the TEG. In addition, in order to decrease the coolant pumping power in the TEG systems, an effective design of the microchannel heat sinks is proposed and implemented in a three-dimensional TEG model [16]. The small thermal conductivity of the thermoelectric materials causes the temperature difference between the cold and the hot surfaces of TEG not to change remarkably when the coolant flow rate varies in the heat sink. Due to the Seebeck effect in the TEG, which transfers a certain amount of energy from high-temperature fluid to electricity, the linear variations in temperature of the fluids in the TEG system are different from the logarithmic variation case in the ordinary parallel-plate heat exchanger [17]. Therefore, the heat flow from the hot source is not equal to the heat flow to the low temperature fluid. Further analysis of the influence of coolant flow rate, heat exchanger geometry, and fluid inlet temperature on the power generation by the TEGs is done by Esartea et al. [18].

Nonetheless, when it comes to real-world design of thermoelectric systems for direct thermal to electricity conversion, a narrow discussion of the TEGs integrated to heat exchangers in micro scale is still lacking. Wojtas et al. [19] reported a complete integration of the microfluidic heat transfer system with a micro-TEG, where the thermoelectric Seebeck voltage is measured as a function of the temperature gradient and applied fluid flow rate. Their demonstration enables us to increase the output power performance of the micro-TEGs. The thermoelectric Seebeck voltage is measured as a function of the applied flow rate and temperature gradient. In this work, a micro plate-fin heat sink that is made of aluminum is applied to a TEG. The purpose is considering the power generation versus the pumping power, which is produced by the pressure loss of the coolant fluid in the system. The particular focus of this experimental study is, exploring the optimum coolant flow rate that results the maximum net-power in the system, at a wide average temperature difference range of the hot and cold sides of the TEG ($\Delta T_{teg,av}$). By considering the average temperature of the hot surfaces of the TEG legs, these optimum points are suggested as the optimum applied pressure drop in the microchannel heat sink by Rezania and Rosendahl [20]. In addition, the temperature distribution and pressure loss in some microchannels with variation of the coolant flow rate and heat flux are reported. Fig. 1 illustrates the schematic, thermocouple and pressure gages location, and the setup of the experiments.

2. Theoretical background

The heat transfer rate removed by the coolant flow in the heat sink is [21]:

$$Q = \dot{m}C_p(T_o - T_i). \tag{1}$$

The pumping power to circulate the coolant flow in the heat sink is related to the pressure drop and the volumetric flow rate, and can be calculated as follows:

$$P_{pump} = \dot{V}\Delta p = \dot{V}(p_o - p_i). \tag{2}$$

The thermal entry length of the internal flow at the laminar regime is approximated by [22]:

$$x_h \approx 0.05 D_h \mathrm{RePr}. \tag{3}$$

where D_h is the hydraulic diameter of a rectangular cross section shape channel defined as follows:

$$D_h = \frac{2wH}{w+H}. \tag{4}$$

The Reynolds number in the channels is [23]:

$$\mathrm{Re} = \frac{\rho u D_h}{\mu}. \tag{5}$$

In this study, the effect of the temperature variation on the thermo-fluid properties of the coolant flow is taken into account. In the TEGs, if the hot and cold junctions are maintained at different temperatures, an open-circuit electromotive force develops between them, and is given by $V = \propto \Delta T$, which defines the differential Seebeck coefficient between the two sides of the elements. Therefore, the power generation is as follows [24]:

$$P_{teg} = IV = \propto^2 \sigma \times \Delta T_{teg}{}^2 \times \frac{A}{L_{teg}}, \tag{6}$$

where $\propto^2 \sigma$ is the power factor of the thermoelectric materials. We define the net-power in the system as follows:

$$P_n = P_{teg} - P_p. \tag{6}$$

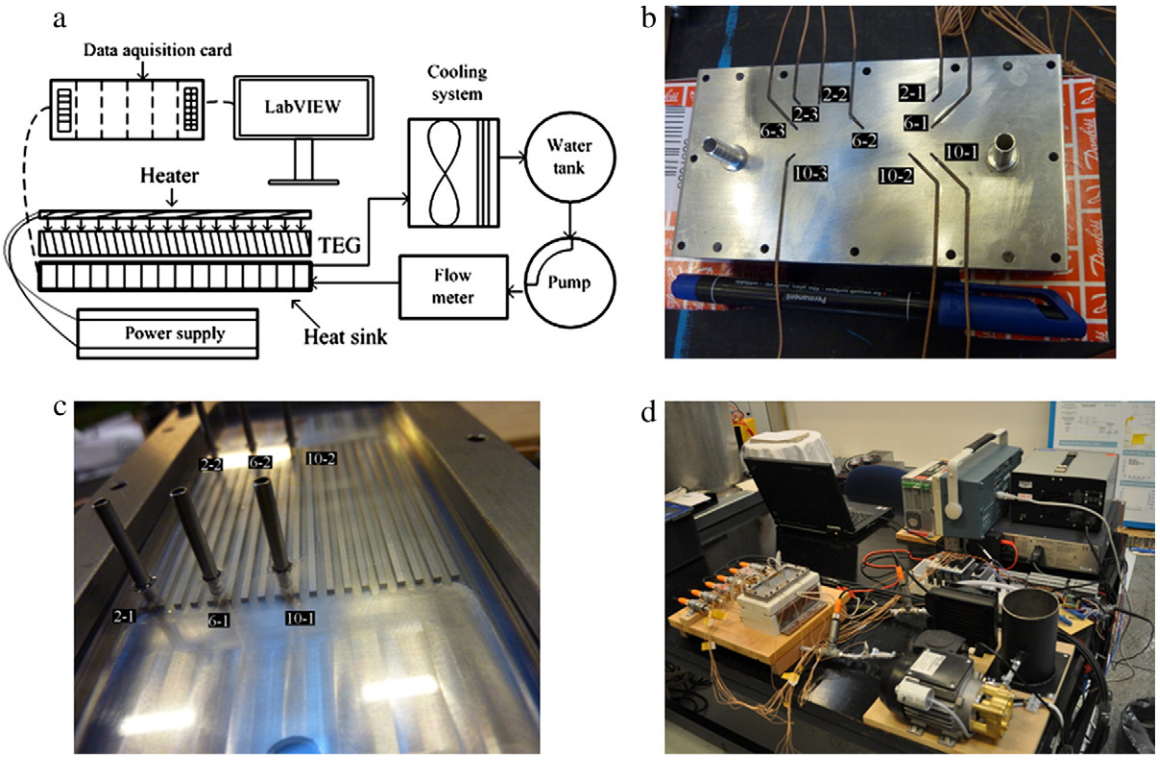

Fig. 1. The geometrical configuration of the system. a. System schematic. b. Thermocouples location. c. Pressure gages location. d. Setup of the experiments.

3. Experimental procedure

The fabricated microchannel heat sink for this work contains twenty rectangular cross section shape microchannels. The inlet and outlet plenums of the heat sink open on the top cover plate, and the coolant flow passes through a U-shape path in the heat sink. Therefore, it is supplied and leaves the heat sink vertically. According to [14], this type of the plenum makes a better uniform velocity distribution in the heat sink, so that it provides better surface temperature uniformity in the heat sink. Base on this uniform mass flow rate distribution in the channels, an average Reynolds number can be valid for the channel through entire the heat sink. The imposed coolant flow rates in this study generate Reynolds number between Re = 63 and Re = 1473. This range of the Reynolds number is lower than the reported critical number by Li et al. [25]. They found that the transition to the turbulence regime began near Re = 1535 in microchannels, which is lower than critical Reynolds number predicted by the classical theory. Therefore, in this study, the maximum imposed flow rate in the heat sink is 1.5l/min. The estimated thermal entry length varies between $x_h = 2.06$ mm for the minimum average Reynolds number (Re = 63) and $x_h = 48$ mm for the maximum average Reynolds number (Re = 1473). Although, the thermal entry length is short at low flow rate but as the flow rate increases, the effect of the thermal entry length cannot be negligible.

In order to measure the temperature variation of the heat sink and the temperature difference of the hot and cold sides of the TEG, T-type thermocouples are used. The thermocouples for measuring the temperature of the coolant fluid in the microchannels are installed in the solid region of the heat sink substrate plate, but close to the fluid region. Since the height of the microchannels is small compared to the channel width, the thermocouples represent an accurate temperature of the bulk fluid in the microchannels. By using eight pressure gages at the inlet and outlet of the heat sink and microchannels #2, #6, and #10 the pressure drop in the heat sink and microchannels are measured. Fig. 1b and c illustrates the thermocouple and pressure gage locations in the heat sink, respectively. The model of the TEG used for this experiment with dimension of 56 × 56 mm is G2-56-0375 made by Tellurex. The voltage and current of the TEG are regulated to give maximum power at any ΔT_{teg}.

The data of this work are recorded at thermally steady state in the system for five $\Delta T_{teg,av}$ (10, 20, 40, 60, and 80 K) and four flow rates (0.07, 0.5, 1.0, and 1.5 l/min) in the heat sink. The ultrasonic flow sensor for water continuous measurement is from Burkert with accuracy of 0.01%. The inlet coolant flow temperature is fixed at 301.5 K and the ambient temperature is approximately constant at 296 K through the experiments. Water is used as the coolant fluid in the heat sink. An appropriate Labview program is applied to record the data of the measurement. The geometry details of the microchannel heat sink is mentioned in Table 1.

4. Results

As Fig. 2 reveals, the pumping power increases with the coolant flow rate with sharper slope compared to the increasing of the output power of the TEG. Although, the imposed heat flux on the hot side of the TEG is constant at each stage of the test, when the coolant flow rate changes, the output power increases with the flow rate. According to a report by Crane et al. [26], at a constant temperature difference of the hot and cold sides of the TEG (ΔT_{teg}), the efficiency of the TEG systems integrated with the heat exchangers increases when the TEG

Table 1
The geometry details of the microchannel heat sink.

Parameter	H_{ch} (μm)	w_{ch} (μm)	t (μm)	D_h (μm)	L_{ch} (mm)	w_{hs} (mm)	L_{pl} (mm)	$D_{pl,i/o}$ (mm)
Dimension	700	1400	1400	933	56	56	50	5.0

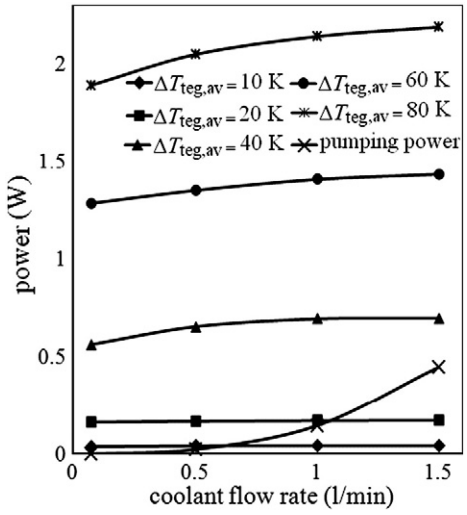

Fig. 2. The power generation in the TEG versus the pumping power.

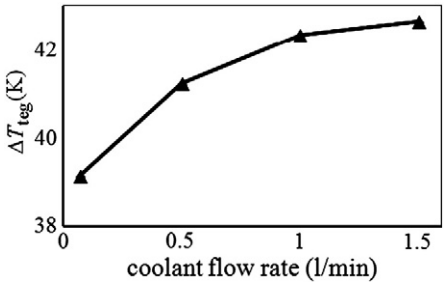

Fig. 3. The ΔT_{teg} variation with the coolant flow rate at fixed heat flux.

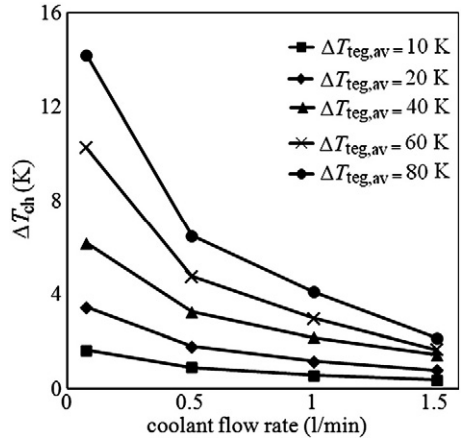

Fig. 4. The variation of the inlet/outlet temperature difference in microchannel #6 with the coolant flow rate.

cold side temperature decreases. Therefore, increasing the coolant flow rate at constant heat flux can result to higher output power.

In addition, as the coolant flow rate in the heat sink increases, the average coolant flow temperature reduces because, the average flow velocity in the channels raises. Therefore, the heat removal capacity of the flow increases, and the hot side temperature of the TEG reduces. When the hot side temperature decreases the heat loss rate through the thermal insulation of the system reduces, so that the higher heat flux crosses through the TEG, and therefore the output power increase. However, the plots in Fig. 2 are shown based on the constant $\Delta T_{teg,av}$, the ΔT_{teg} varies slowly with the coolant flow rate. This variation can

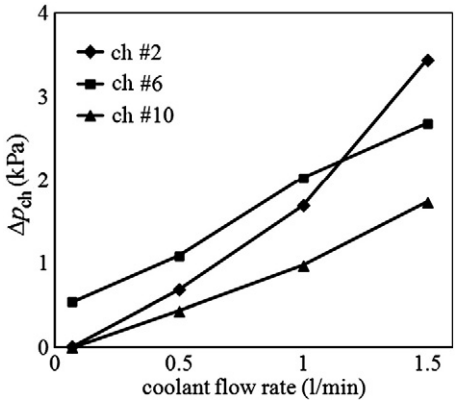

Fig. 5. The variation of the pressure loss in microchannels #2, #6, and #10 with the coolant flow rate.

be noticed in Fig. 3 for a sample $\Delta T_{teg,av}$. As is reported by Wojtas et al. [19], the reason of the small variation of the ΔT_{teg} lies in the relatively small impact decreasing of the thermal resistance of the heat sink compared to the absolute value.

As is expected, the inlet/outlet temperature difference of the coolant fluid in the microchannels decreases with the thermal resistance of the heat sink, due to rising of the flow rate. In addition for sample microchannel #6, Fig. 4 shows that the temperature difference of the coolant fluid increases with the $\Delta T_{teg,av}$. The inlet/outlet arrangement effect of the plenums on the coolant flow distribution is shown in Fig. 5. The pressure loss in the middle channels reveals linear behavior when the flow rate varies. But the pressure drop variation in microchannel #2, which is fabricated at the side of the heat sink, has increased exponentially with the flow rate. Therefore, the distributed rate of the flow is higher in the microchannels at the sides of the heat sink than the flow in the microchannels in the middle of the heat sink, as is shown by Chein and Chen [14].

It can be seen in Fig. 2 that higher $\Delta T_{teg,av}$ and coolant flow rate produce higher output power in the TEG. On the other hand, the pumping power increases with the rising of the flow rate in the heat sink and may decrease the net-power generation from the system. Therefore, there should be a unique optimum flow rate at every $\Delta T_{teg,av}$ that gives maximum net-power. These optimum points are revealed in Table 2. The flow rate equal to 0.5 l/min gives the maximum net-power among the other tested flow rates in this work for the $\Delta T_{teg,av} \geq 40$ K. At the smaller $\Delta T_{teg,av}$, lower flow rate can produce maximum net-power. It is expected that when the $\Delta T_{teg,av}$ increases, the optimum flow rate that results maximum net-power shifts to higher value.

5. Conclusions

A microchannel heat sink is applied to a TEG in order to make a light and compact energy system. The power generated versus the coolant pumping power is studied in the TEG. Additionally, the optimum coolant flow rates that result in the maximum net-power in the system are explored. The results show that there is a unique coolant flow rate at any $\Delta T_{teg,av}$ that makes maximum net-power in the system. The value of the optimum flow rate increases when the $\Delta T_{teg,av}$ increases.

Table 2
The net-power generation at the studied coolant flow rates.

	$\Delta T_{teg,av}$				
Flow rate (1/min)	10 K	20 K	40 K	60 K	80 K
0.07	0.035	0.164	0.562	1.282	1.890
0.5	0.018	0.146	0.632	1.320	2.026
1.0	−0.103	0.027	0.551	1.263	1.996
1.5	−0.406	−0.275	0.250	0.970	1.741

Results also reveal that the temperature difference of the hot and cold sides of the TEG increase slowly with the flow rate at a constant imposed heat flux. The reason of this small variation lies in the relatively small impact decreasing of the thermal resistance of the heat sink.

Acknowledgments

This work was carried out within the framework of the Center for Energy Materials and is funded in part by the Danish Council for Strategic Research, Programme Commission on Energy and Environment, under grant no 823032. The authors would like to thank Dr. Ali Enkeshafi, Jan Christiansen, and Jens Korsgaard for all their kind assistance and support.

References

[1] B. Agostini, M. Fabbri, J.E. Park, L. Wojtan, J.R. Thome, B. Michel, State of the art of high heat flux cooling technologies, Heat Transfer Engineering 28 (2007) 258–281.
[2] E. Raj, Z. Lisik, M. Langer, G. Tosik, J. Wozny, The numerical approach to analysis of microchannel cooling systems, ICCS 2005, LNCS 3514 (2005) 876–883.
[3] P. Rosa, T.G. Karayiannis, M.W. Collins, Single-phase heat transfer in microchannels: the importance of scaling effects, Applied Thermal Engineering 29 (2009) 3447–3468.
[4] A. Rezania, L.A. Rosendahl, Evaluating thermoelectric power generation device performance using a rectangular microchannel heat sink, Journal of Electronic Materials 40 (2011) 481–488.
[5] G.P. Celata, M. Cumo, M. Guglielmi, G. Zummo, Experimental investigation of hydraulic and single phase heat transfer in 0.130 mm capillary tube, In: in: G.P. Celata, et al., (Eds.), Int. Conf. Heat Transfer and Transport Phenomena in Microscale, 2000, pp. 108–113.
[6] B.X. Wang, X.F. Peng, Experimental investigation on liquid forced convection heat transfer through microchannels, International Journal of Heat and Mass Transfer (Suppl. 37) (1994) 73–82.
[7] S.B. Choi, R.F. Barron, R.O. Warrington, Fluid flow and heat transfer in microtubes, micromechanical sensors, actuators and systems, ASME DSC 32 (1991) 123–134.
[8] C.Y. Yang, H.T. Chien, S.R. Lu, R.J. Shyu, Friction characteristics of water, R134a and air in small tubes, In: in: G.P. Celata, et al., (Eds.), Int. Conf. Heat Transfer and Transport Phenomena in Microscale, 2000, pp. 168–174.
[9] X.F. Peng, G.P. Peterson, Convective heat transfer and flow friction for water flow in microchannel structures, International Journal of Heat and Mass Transfer 39 (1996) 2599–2608.
[10] P. Gunnasegaran, H.A. Mohammed, N.H. Shuaib, R. Saidur, The effect of geometrical parameters on heat transfer characteristics of microchannels heat sink with different shapes, International Journal of Heat and Mass Transfer 37 (2010) 1078–1086.
[11] Y. Chen, C. Zhang, M. Shi, J. Wu, Three-dimensional numerical simulation of heat and fluid flow in noncircular microchannel heat sinks, International Communications in Heat and Mass Transfer 36 (2009) 917–920.
[12] C.J. Kroeker, H.M. Soliman, S.J. Ormiston, Three-dimensional thermal analysis of heat sinks with circular cooling micro-channels, International Journal of Heat and Mass Transfer 47 (2004) 4733–4744.
[13] D.B. Tuckerman, R.F.W. Pease, High-performance heat sinking for VLSI, IEEE Electron Device Letters 2 (1981) 126–129.
[14] R. Chein, J. Chen, Numerical study of the inlet/outlet arrangement effect on microchannel heat sink performance, International Journal of Thermal Sciences 48 (2009) 1627–1638.
[15] A. Martinez, J.G. Vian, D. Astrain, A. Rodriguez, I. Berrio, Optimization of the heat exchangers of a thermoelectric generation system, Journal of Electronic Materials 39 (2010) 1463–1468.
[16] A. Rezania, L.A. Rosendahl, New configurations of micro plate-fin heat sink in order to reduce coolant pumping power, To be published on J. Electronic Materials, DOI: 10.1007/s11664-011-1887-3 (2012).
[17] J. Yu, H. Zhao, A numerical model for thermoelectric generator with the parallel-plate heat exchanger, Journal of Power Sources 172 (2007) 428–434.
[18] J. Esartea, G. Minb, D.M. Rowe, Modelling heat exchangers for thermoelectric generators, Journal of Power Sources 93 (2001) 72–76.
[19] N. Wojtas, E. Schwyter, W. Glatz, S. Kühne, W. Escher, C. Hierold, Power enhancement of micro thermoelectric generators by microfluidic heat transfer packaging, Sensors and Actuators A: Physical, In Press, Corrected Proof, http://dx.doi.org/10.1016/j.sna.2011.12.043.
[20] A. Rezania, L.A. Rosendahl, Thermal effect of a thermoelectric generator on parallel microchannel heat sink, Energy 37 (2012) 220–227.
[21] R. Chein, Y. Chen, Performances of thermoelectric cooler integrated with microchannel heat sinks, International Journal of Refrigeration 28 (2005) 828–839.
[22] Y. Wang, G.-F. Ding, S. Fu, Highly efficient manifold microchannel heat sink, Electronics Letters 43 (2007) 978–980.
[23] B.X. Wang, X.F. Peng, Experimental investigation on liquid forced convection heat transfer through microchannels, Int. J. Heat and Mass Transfer 37 (1994) 73–82.
[24] D. M. Rowe, Ph.D., D.Sc (Editor), Macro to Nano, Taylor & Francis Group, LLC, 2006.
[25] H. Li, R. Ewoldt, M.G. Olsen, Turbulent and transitional velocity measurements in a rectangular microchannel using microscopic particle image velocimetry, Experimental Thermal and Fluid Science 29 (2005) 435–446.
[26] D.T. Crane, G.S. Jackson, Optimization of cross flow heat exchangers for thermoelectric waste heat recovery, Energy Conversion and Management 45 (2004) 1565–1582.